DOI: https://doi.org/10.57233/ijsgs.v12i3.1199 ISSNp: 2488-9229; ISSNe: 3027-1118

IJSGS FUGUSAU VOL. 12(3) WEBSITE: https://fugus-ijsgs.com.ng

INTERNATIONAL JOURNAL OF SCIENCE FOR GLOBAL SUSTAINABILITY
(A PUBLICATION OF FACULTY OF SCIENCE, FEDERAL UNIVERSITY GUSAU, NIGERIA)

Isotherm, Kinetics and Thermodynamic Studies of Congo Red Dye Adsorption onto Zeolite/Activated Carbon Hybrid Adsorbent

Hawawu Salami[1, 2], Abdullahi Mohammed Evuti[1,3], Yahaya Sayyadi Mohammad[1,4,*]

[1]Department of Chemical Engineering, University of Abuja, Abuja, Nigeria
[2]Department of Chemical Engineering, Kaduna Polytechnic, Kaduna, Nigeria
[3]Leadership University, Kuje-Abuja, Nigeria
[4]Ibrahim Badamasi Babangida University, Lapai, Niger State, Nigeria

***Corresponding author's email:** yahsaymoh@yahoo.co.uk

Received on: August, 2026 **Revised and Accepted on:** September, 2026 **Published on:** October, 2026

ABSTRACT

The rapid growth of industrial activities has significantly increased the volume of wastewater discharged into natural water bodies, creating serious environmental and public health challenges worldwide. This study focused on the application of Zeolite Y/Coconut Shell Activated Carbon (CSAC) hybrid adsorbent for the removal of Congo Red Dye from textile wastewater. Activated carbon was produced from coconut shell through phosphoric acid activation and subsequently combined with zeolite at different proportions to produce hybrid adsorbents, through mechanical mixing and wet impregnation method. Batch experiment was carried out to study the effect of process variables (adsorbent dosage, contact time, solution pH, and temperature) on adsorption of Congo Red Dye onto the hybrid adsorbents. Adsorption isotherm, kinetics and thermodynamic models were employed to analyse the experimental data obtained from the batch adsorption study. The study revealed that the adsorbents effectively removed the investigated dye from aqueous solution, recording removal efficiency of 91.36 % at adsorbent dosage of 0.8 g/50 mL, pH of 4, contact time of 60 mins and temperature of 25 ^{o}C and a monolayer adsorption capacity of 30.2 mg/g. The adsorption process was found to follow Langmuir isotherm and Pseudo-second-order kinetic models. Thermodynamic studies revealed exothermic and non-spontaneous behaviour; however, the reaction was found to be feasible at low temperature.

Keywords: Congo red, Adsorbent, Zeolite, Hybrid, Wastewater

1.0 INTRODUCTION

Industrial wastewater pollution has become a global environmental challenge, with textile effluents posing significant risks due to their high content of synthetic dyes, surfactants, salts, and heavy metals. During dyeing operations, up to 20% of dyes remain unbound to fibres and enter wastewater streams, impairing water quality and aquatic ecosystems (Mnyango *et al.*, 2025). Synthetic dyes, particularly azo dyes, resist degradation by conventional biological and chemical processes, making their removal a priority in sustainable wastewater management (Gayathri *et al.*, 2026). Congo red is widely used in textile processing for its strong affinity to cellulosic fibres and vivid colour intensity. Its molecular structure, comprising azo bonds, benzidine rings, and sulfonate groups, confers high solubility and chemical stability, but also persistence in aquatic environments. Beyond environmental concerns, Congo red poses health risks including mutagenicity, carcinogenicity, and organ toxicity. Under anaerobic conditions, its azo bonds may cleave, forming aromatic amines, compounds known for their carcinogenic potential (Khan *et al.*, 2021; Schmidt *et al.*, 2019; Xiong *et al.*, 2021). These properties underscore the urgency of developing effective removal strategies.

Several treatment technologies have been investigated, including coagulation-flocculation, membrane separation, advanced oxidation, photocatalysis, electrochemical methods, ion exchange, and biological degradation. While these approaches can achieve dye removal under specific conditions, they are often constrained by high costs, sludge generation, incomplete degradation, and operational complexity (Fernandes de Magalhaes *et al.*, 2022). Adsorption has therefore gained attention as a versatile and efficient technique. It offers simplicity, cost-effectiveness, and high removal efficiency without producing secondary pollutants (Chakraborty *et al.*, 2022). Activated carbon remains the benchmark adsorbent due to its large surface area, porous network, and functional groups. However, limitation such as restricted ion-exchange property necessitate further innovation (Tan *et al.*, 2017). Hybrid adsorbents combining activated carbon with zeolites have emerged as promising solutions. Zeolite Y, a crystalline aluminosilicate, offers high surface area, ion-exchange capacity, and structural stability. Its microporous framework, however, can restrict access to bulky dye molecules like Congo Red. Integrating activated carbon with Zeolite Y addresses these limitations by enhancing pore connectivity, broadening the pore-size distribution, and improving the accessibility of adsorption sites. Activated carbon facilitates transport of large dye molecules, while zeolite contributes ion-exchange capacity.

Adsorption of Congo Red onto these hybrids involves multiple mechanisms: electrostatic attraction between dye sulfonate groups and positively charged adsorbent sites, π–π interactions with carbon's aromatic domains, hydrogen bonding, van der Waals forces, pore filling, and ion exchange (Arias *et al*., 2026). The relative contribution of each mechanism depends on operational parameters such as pH, contact time, dye concentration, adsorbent dosage, and temperature. A comprehensive evaluation of adsorption requires equilibrium, kinetic, and thermodynamic analyses. Together, these analyses clarify the feasibility and driving forces of adsorption, guiding optimization for industrial applications. Although extensive research has examined Congo Red adsorption using activated carbon, zeolites, agricultural wastes, and other low-cost adsorbents, relatively few studies have focused on coconut shell-derived activated carbon combined with Zeolite Y at varying ratios.

This study therefore investigates the adsorption behaviour of Congo red onto Zeolite Y/Coconut Shell Activated Carbon hybrids through equilibrium isotherms, kinetic modelling, and thermodynamic analysis. By examining these parameters, the research aims to elucidate adsorption mechanisms, assess spontaneity and feasibility, and provide insights for optimizing hybrid adsorbents in industrial wastewater remediation.

2.0 MATERIALS AND METHODS

2.1 Materials

Materials used include Orthophosphoric acid (H_3PO_4,) with 98% purity, analytical grade Sodium hydroxide (NaOH) and Hydrochloric acid (HCl) (BDH Chemicals), Congo red ($C_{32}H_{22}N_6Na_{2O6}S_2$; molecular weight: 696.66 g/mol) and all chemical reagents were of analytical grade. Faujasite-type Zeolite Y was sourced from Kaduna Refining and Petrochemical Company (KRPC), Kaduna, Nigeria.

2.2 Preparation of Activated Carbon from Coconut Shell

Coconut shells were collected from Bakindogo Central Market, Kaduna State, Nigeria. The shells were thoroughly washed with tap water to remove foreign materials, followed by rinsing with distilled water, and then sun-dried for five days, and later oven-dried overnight. Thereafter, dried shells were crushed with an industrial crusher and grinding machine (Olatunji *et al*., 2024). The resulting powder was sieved through a 280 µm mesh to obtain a uniform particle size. Activated carbon was prepared following a modified method of Onigemo *et al*. (2024). The sieved coconut shell powder was placed in crucibles and carbonized in a muffle furnace at 500 °C for 1 hour. After cooling in a desiccator, the carbonized material was impregnated with 1 M phosphoric acid solution at a ratio 2:1 for 24 hours at room temperature (Oyedoh and Igbokwe, 2025). The impregnated samples were washed with distilled water until a neutral pH was achieved, then activated at 350 °C for 2 hours in a furnace (Olatunji *et al*., 2024). Finally, the samples were oven-dried overnight at 120 °C, cooled in a desiccator, and stored in airtight labelled container for subsequent blending with zeolite Y to form hybrid adsorbents.

2.3 Formulation of Zeolite Y/Coconut Shell Activated Carbon (CSAC) Hybrid

The Zeolite/CSAC hybrid adsorbent was prepared by mechanical mixing followed by wet impregnation (Dryaz *et al*., 2021; Mohamed *et al*., 2022). Particle-size analysis was conducted on both zeolite and activated carbon, and samples were milled and sieved to 150 µm (Nwafulugo, 2014). Specific weight ratios were measured and blended using a domestic blender to ensure homogeneity. To enhance bonding between zeolite and activated carbon, the blends were mixed with distilled water at a ratio of 1:10 (Dryaz *et al*., 2021) and stirred at 500 rpm for 60 minutes using a magnetic stirrer. The mixture was further treated in a water bath at 300 rpm for 60 minutes at room temperature. The resulting hybrid adsorbent was filtered, washed repeatedly with distilled water to remove unreacted ions, and oven-dried at 60 °C for 24 hours. The dried hybrid samples labelled as Sample 2 (20% Zeolite + 80% CSAC), Sample 3 (50% Zeolite + 50% CSAC) and Sample 4 (80% Zeolite + 20% CSAC), were stored in airtight containers for batch adsorption experiments.

2.4 Batch Adsorption Studies

The adsorption experiment was carried out using all the prepared hybrid adsorbent samples (Sample A, B and C). Standard solution of Congo red was prepared. Adsorbent dosages of 0.2, 0.4, 0.6, 0.8, and 1 g were weighed into 100 mL shaker flasks. 50 mL of 500 mg/L dye solution was weighed into each flask. Samples were agitated at 250 rpm, 25 °C, and pH of 6 for 30 minutes. Mixtures were filtered using Whatman filter paper, and residual dye concentrations were measured with a UV spectrophotometer. The process variables studied are; adsorbent dosage (0.2-1g), Solution pH (4-12) adjusted using 0.1 mol/L HCl or NaOH, contact time (30-120 min) and temperature (25, 30, 40, 50 and 60 °C). All treatments were replicated for accuracy. This procedure was repeated for all hybrid adsorbent samples to evaluate adsorbent performance. Adsorption capacity (q_e) and Removal efficiency (RE) were calculated using equations 1 and 2, respectively:

$$q_e = \frac{(C_o - C_e)V}{m} \quad (1)$$

$$\text{RE} = \frac{(C_o - C_f)}{C_o} \times 100 \quad (2)$$

where: q_e= equilibrium adsorption capacity (mg/g), RE= removal efficiency (%), C_o, C_e, C_f= initial, equilibrium, and final dye concentrations (mg/L), V= solution volume (mL) and m= adsorbent mass (g)

DOI: https://doi.org/10.57233/ijsgs.v12i3.1199 ISSNp: 2488-9229; ISSNe: 3027-1118
IJSGS FUGUSAU VOL. 12(3) WEBSITE: https://fugus-ijsgs.com.ng

2.5 Adsorption Isotherm Study

Langmuir isotherm model

The linearized form of Langmuir isotherm model (equation 3) was used by plotting $\frac{C_e}{q_e}$ against C_e. Equilibrium isotherm parameters for the model were obtained from the slope and intercept of the plot:

$$\frac{C_e}{q_e} = \frac{1}{bQ_m} + \frac{C_e}{Q_m} \quad (3)$$

Freundlich isotherm model

The linearized form of the Freundlich isotherm model given in equation 4 was used by plotting $\log q_e$ against $\log C_e$. Equilibrium isotherm parameters for the model were also obtained from the slope and intercept of the plot:

$$\log q_e = \log K_f + \frac{1}{n}\log C_e \quad (4)$$

Where: q_e = adsorption capacity at equilibrium (mg/g), C_e = equilibrium concentration of solute (mg/L), Q_m = maximum monolayer adsorption capacity (mg/g), b = Langmuir isotherm constant (dm^3/mg), K_f = Freundlich isotherm constant (mg/g), and n = adsorption intensity

2.6 Adsorption Kinetic Study

Pseudo-first-order kinetic (PFO) model

The linearized form of pseudo-first-order kinetic model in equation 5 was used by plotting $\log(q_e - q_t)$ against *t*. Kinetic parameters for the model were obtained from the slope and intercept of the plot:

$$\log(q_e - q_t) = \log q_e - \frac{k_1}{2.303}t \quad (5)$$

Pseudo-second-order kinetic (PSO) model

The linearized form of pseudo-second-order kinetic model given in equation 6 was used by plotting $\frac{t}{q_t}$ against *t*. Kinetic parameters for the model were obtained from the slope and intercept of the plot:

$$\frac{t}{q_t} = \frac{1}{k_2 q_e^2} + \frac{1}{q_e}t \quad (6)$$

Where: q_t = adsorption capacity at time *t* (mg/g), q_e = adsorption capacity at equilibrium (mg/g), t = time (min), k_1 = PFO kinetic rate constant (min^{-1}), and k_2 = PSO kinetic rate constant (g mg^{-1} min^{-1})

2.7 Adsorption Thermodynamic Study

The thermodynamic model (Van't Hoff equation) in equation 7 was used by plotting $\ln k_d$ against $1/T$. Thermodynamic parameters for the model were obtained from the slope and intercept of the plot:

$$\ln k_d = \frac{\Delta S^o}{R} - \frac{\Delta H^o}{RT} \quad (7)$$

And the Gibbs free energy was determined from equation 8:

$$\Delta G^o = -RTIn\ k_d \quad (8)$$

Where: k_d = thermodynamic equilibrium constant ($k_d = \frac{q_e}{C_e}$), q_e = adsorption capacity at equilibrium (mg/g), C_e = equilibrium concentration of solute (mg/L), T = absolute temperature (K), and R = gas constant (8.314 J/mol K)

3.0 RESULTS AND DISCUSSION

3.1 Effect of Process Variables

Effect of Adsorbent Dosage

The effect of adsorbent dosage was investigated at 0.2–1.0 g/50 mL under controlled conditions (25 °C, pH 6, 30 min contact time). Result (Figure 1) showed that removal efficiency increased with adsorbent dosage across all adsorbent samples, due to the availability of more surface area and active sites for adsorption (Senol *et al.*, 2024). However, the magnitude and pattern of removal varied depending on adsorbent composition. The removal efficiency increased sharply between 0.2 g and 0.8 g, then plateaued, likely due to particle agglomeration that reduced the effective surface area (Javeda *et al.*, 2024). The removal efficiencies ranged from 22.23-74.08% (Sample 2), 17.93-71.7% (Sample 3), and 14.9-62.2% (Sample 4). The highest efficiency demonstrated by Sample 2 is attributed to its high activated carbon content, which provides a porous aromatic structure that facilitates π–π interactions with the large anionic dye molecules. However, Sample 3 showed moderate performance, while Sample 4, with higher zeolite content, was the least effective for Congo Red removal. Furthermore, the adsorption capacity (Figure 2) was noted to decrease with increasing adsorbent dosage for the adsorption of Congo red dye. This behaviour is commonly observed in adsorption systems as increasing the adsorbent dosage provides more adsorption sites than are required for the available dye molecules, resulting in lower dye uptake per unit mass of adsorbent. Thus, adsorbent dosage of 0.8g was chosen as the optimal value for subsequent experiment.

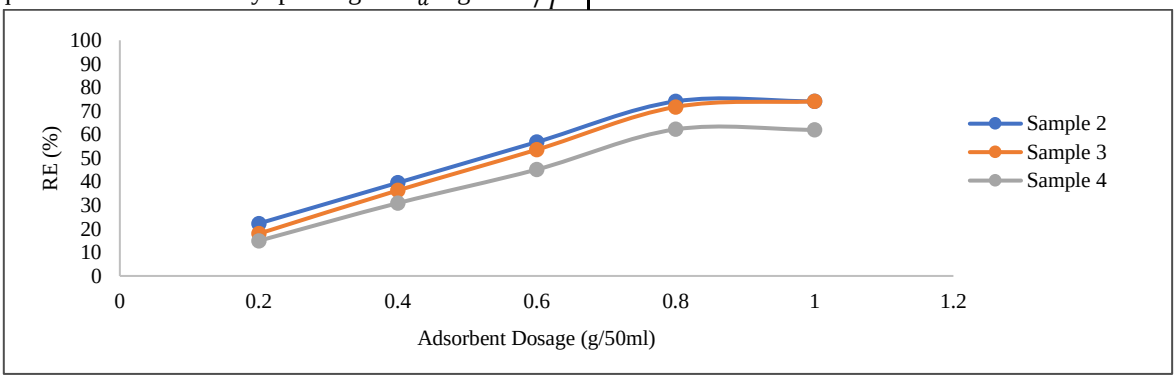

Figure 1: Effect of adsorbent dosage on the removal of Congo red by hybrid adsorbents (25 °C, pH 6, 30 min contact time)

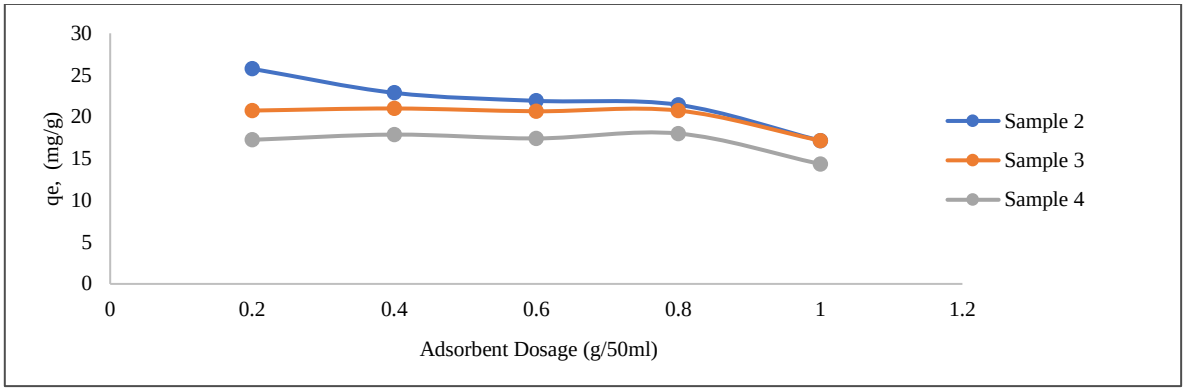

Figure 2: Effect of adsorbent dosage on the adsorption capacity of the hybrid adsorbents for Congo red Removal (25 °C, pH 6, 30 min contact time)

Effect of solution pH

The pH of the solution plays a critical role in adsorption studies, as it influences both the surface charge of the adsorbents and the ionization or speciation of the adsorbate (Jaramillo-Fierro *et al*., 2023). The point of zero charge (pH_{PZC}) is particularly important in assessing adsorption efficiency, since it determines whether the adsorbent surface is positively or negatively charged under any given conditions. The pH_{PZC} values of the prepared hybrid adsorbents were found to be 5.1, 5.3, and 6.8 for Samples 2, 3, and 4, respectively (Figure 3). At pH values above these thresholds, the adsorbent surfaces acquire a net negative charge due to deprotonation of surface functional groups, favouring adsorption of cationic species. Conversely, at pH values below the pH_{PZC}, protonation occurs, conferring a net positive charge that enhances adsorption of anionic species (Tubon-Usca *et al*., 2025).

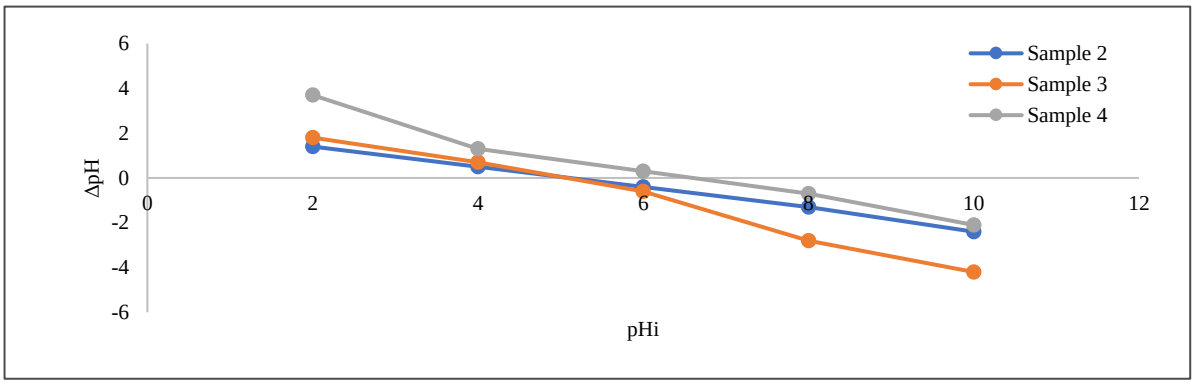

Figure 3: pH at the point of zero charge (pH_{PZC}) for all the samples

The pH range of 4-12 was used as these pH values cover the full spectrum from strongly acidic to alkaline conditions found in industrial effluents. Congo red adsorption was strongly pH-dependent, with maximum removal observed under acidic conditions as illustrated in Figure 4. As pH increased from 4 to 8, removal efficiency decreased sharply, with values dropping from 80.56 to 38.88% (Sample 2), 76.24 to 23.76% (Sample 3), and 67.60 to 20.09% (Sample 4). Beyond pH 8, adsorption was negligible. This behaviour is explained by electrostatic repulsion between negatively charged adsorbent surfaces (above pH_{PZC}) and the anionic dye molecules (Alawam *et al*., 2025). Sample 2, with the higher activated carbon content, exhibited the best performance due to π–π interactions and favourable surface chemistry, while Sample 4, rich in zeolite Y, showed the lowest efficiency. Thus, the optimal pH for dye removal is 4. As illustrated in Figure 5, solution pH had a pronounced effect on the adsorption capacity of the adsorbents as there was a decrease in adsorption capacities with increasing pH.

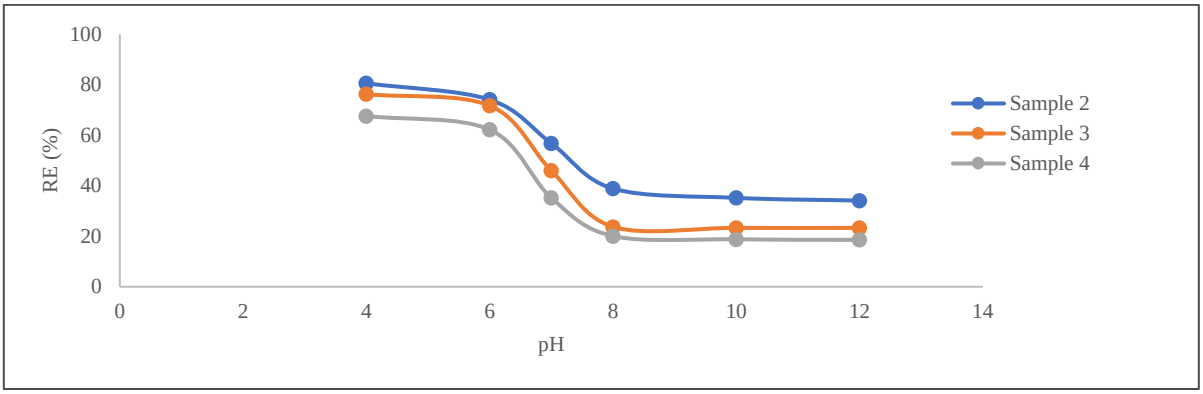

Figure 4: Effect of pH on the removal of Congo red by hybrid adsorbents (25 °C, adsorbent dose of 0.8/50 ml, 30 min contact time)

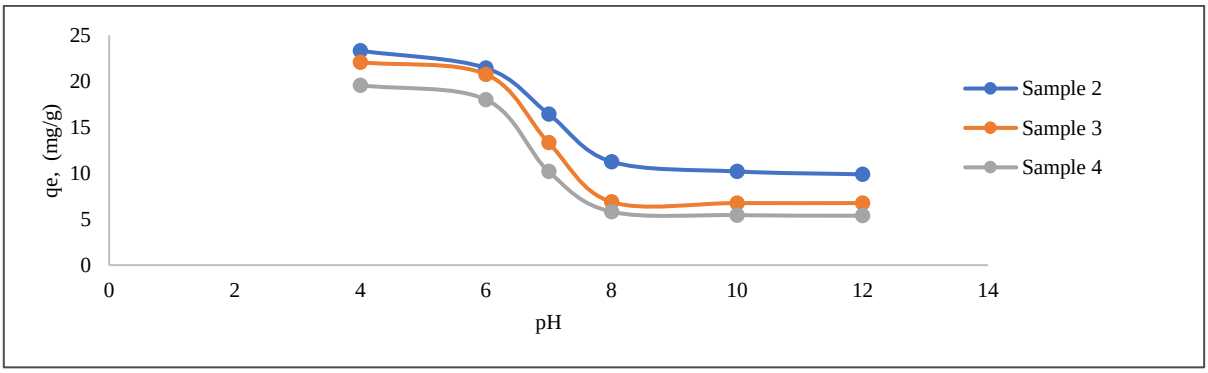

Figure 5: Effect of pH on the adsorption capacity of the hybrid adsorbents for Congo red Removal (25 °C, adsorbent dose of 0.8/50 ml, 30 min contact time)

Effect of Contact Time

Contact time is a critical factor in adsorption studies, as it determines the extent of dye molecules interaction with available active sites on the adsorbent surface. The result as presented in Figure 6, shows that adsorption efficiency generally increased with time due to the strong driving force for mass transfer, large surface area, and the availability of numerous active sites. However, once equilibrium is reached, no significant improvement was observed, likely due to saturation of active sites at prolonged contact times (Gkika *et al*., 2025). The adsorption of Congo red was rapid during the first 60 minutes, after which the rate slowed. Equilibrium was reached between 60-80 minutes for Samples 2 and 4, and at approximately 90 minutes for Sample 3, as shown in Figure 6. The rapid initial adsorption is explained by the high number of vacant sites available for dye binding.

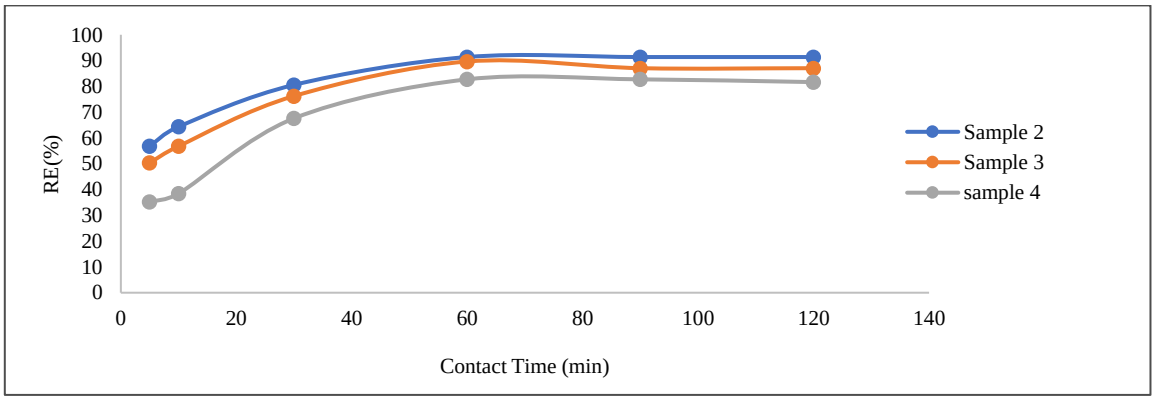

Figure 6: Effect of Contact Time on the removal of Congo red by hybrid adsorbents (25 °C, adsorbent dose of 0.8/50 ml, pH of 4)

DOI: https://doi.org/10.57233/ijsgs.v12i3.1199 ISSNp: 2488-9229; ISSNe: 3027-1118
IJSGS FUGUSAU VOL. 12(3) WEBSITE: https://fugus-ijsgs.com.ng

Effect of Temperature

Figure 7 revealed that as the temperature was increased from 25 to 60 °C, the removal efficiencies of Congo red gradually decreases for all adsorbents, indicating exothermic behaviour. This trend aligned with the works of Dryaz *et al*. (2021); El Jery *et al*. (2024). The decline in the adsorption of Congo red with increasing temperature suggests that higher temperatures reduce the strength of the attractive forces between the dye molecules and the adsorbent surface. The increase in molecular kinetic energy at elevated temperatures promotes desorption and weakens the interactions responsible for adsorption, resulting in lower removal efficiencies (Dryaz *et al*., 2021).

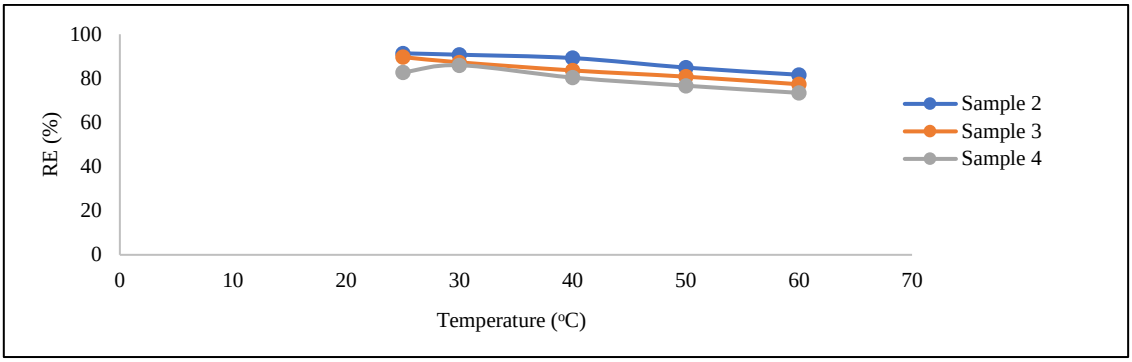

Figure 7: Effect of Temperature on the removal of Congo red by hybrid adsorbents (adsorbent dose of 0.8/50 ml, 60 min contact time, pH of 4)

3.2 Adsorption Isotherms

The Langmuir model assumes monolayer adsorption on a homogeneous surface with no adsorbate–adsorbate interactions. The parameters obtained as presented in Table 1 reveal significant variation in monolayer adsorption capacity (q_m) and affinity constant (b). Sample 2 showed the highest q_m (30.21 mg/g), followed by Sample 3 (22.08 mg/g) and Sample 4 (18.87 mg/g). High R^2 values (0.9708–0.9916) across all samples confirm that Congo Red adsorption is well described by the Langmuir model, indicating strong adsorbate-adsorbent interactions and monolayer coverage. The Langmuir affinity constant (b) further supports these observations. This further confirms the strong attraction between the dye molecules and the surface of the adsorbents. This observation is in agreement with the trend reported by Deng *et al*. (2022); Wongcharee *et al*. (2018). The separator factor R_L is used in identifying the favorability of the adsorption process; thus, when $R_L>1$ is unfavorable, $R_L=1$ is linear, $0<R_L<1$ is favorable, and irreversible when $R_L = 0$ (Ayawei *et al*., 2017). The separation factor (R_L) values for all systems were less than 1, confirming favourable adsorption under the studied conditions which aligned with the work of Wongcharee *et al*. (2018). The Freundlich model, which accounts for adsorption on heterogeneous surfaces and multilayer formation, showed comparatively lower R^2 values than the Langmuir model, indicating a less satisfactory fit overall.

Table 1. Adsorption Isotherm Models Data

Model	Parameter	Sample 2	Sample 3	Sample 4
Langmuir	Q_m(mg/g)	30.212	22.075	18.868
	b (L/g)	0.014	0.051	0.036
	R_L	0.137	0.041	0.057
	R^2	0.9708	0.9916	0.9632
Freundlich	1/n	0.25	0.108	0.113
	n	4.003	9.294	8.857
	k_f (L/g)	5.789	11.272	9.068
	R^2	0.6968	0.3895	0.1879

DOI: https://doi.org/10.57233/ijsgs.v12i3.1199 ISSNp: 2488-9229; ISSNe: 3027-1118

IJSGS FUGUSAU VOL. 12(3) WEBSITE: https://fugus-ijsgs.com.ng

The adsorption capacity (q_e) was evaluated using the Langmuir isotherm model. Predicted values (q_{calc}) were compared with experimental data (q_{expt}) to assess the suitability of the model in describing the adsorption process. The degree of agreement between calculated and experimental values provided insight into the adsorption mechanisms. The results presented in Tables 2 confirmed that the Langmuir model closely matches experimental results, with few exceptions, particularly at low to moderate adsorbent dosages.

Table 2: Experimental Adsorption Capacity versus Calculated Adsorption Capacity

Mass (g)	Sample 2		Sample 3		Sample 4	
	$q_{e,expt}$ (mg/g)	$q_{e,calc}$ (mg/g)	$q_{e,expt}$ (mg/g)	$q_{e,calc}$ (mg/g)	$q_{e,expt}$ (mg/g)	$q_{e,calc}$ (mg/g)
0.2	25.75	25.087	20.75	20.994	17.25	17.616
0.4	22.875	23.928	21.00	20.702	17.875	17.349
0.6	21.917	22.090	20.667	20.233	17.417	16.994
0.8	21.438	18.733	20.75	19.206	18.00	16.265
1.0	17.15	18.733	17.15	18.98	14.35	16.277

3.3 Adsorption Kinetics

Adsorption kinetics studies provide valuable insights into the mechanism and rate-controlling steps of dye uptake. The results presented in Tables 3 revealed that while both models provided good fits, the Pseudo-second-order (PSO) kinetic model provided better fits across all adsorbent samples, with R^2 values approaching unity (0.9853–0.9999). The PSO model yielded high adsorption capacities, with Sample 2 (27.55 mg/g) slightly outperforming Samples 3 and 4. It was observed from Table 4 that the PSO model consistently provides more accurate predictions than the Pseudo-first-order (PFO) model.

Table 3. Adsorption Kinetic Models Data

Model	Parameters	Sample 2	Sample 3	Sample 4
PFO	q_e (mg/g)	12.52	13.954	18.8538
	K_1 (min^{-1})	0.046	0.05	0.048
	R^2	0.9998	0.9982	0.9819
PSO	q_e (mg/g)	27.548	26.455	26.042
	K_2 (g mg^{-1} min^{-1})	0.0089	0.0081	0.0041
	R^2	0.9994	0.9983	0.9956

DOI: https://doi.org/10.57233/ijsgs.v12i3.1199 ISSNp: 2488-9229; ISSNe: 3027-1118
IJSGS FUGUSAU VOL. 12(3) WEBSITE: https://fugus-ijsgs.com.ng

Table 4: Experimental Adsorption Capacity versus Calculated Adsorption Capacity

Model	Time (min)	Sample 2		Sample 3		Sample 4	
		$q_{t,expt}$ (mg/g)	$q_{t,calc}$ (mg/g)	$q_{t,expt}$ (mg/g)	$q_{t,calc}$ (mg/g)	$q_{t,expt}$ (mg/g)	$q_{t,calc}$ (mg/g)
PFO	5	16.438	2.587	14.563	3.0703	10.188	4.030
	10	18.625	4.64	16.438	5.465	11.125	7.199
	30	23.313	9.398	22.063	10.812	19.563	14.400
	60	26.438	11.742	25.938	13.247	23.938	17.802
	90	26.438	12.326	25.188	13.795	23.938	18.605
	120	26.438	12.472	25.188	13.918	23.625	18.795
PSO	5	16.438	15.172	14.563	13.684	10.188	9.064
	10	18.625	19.567	16.438	18.038	11.125	13.447
	30	23.313	24.251	22.063	22.894	19.563	19.846
	60	26.438	25.795	25.938	24.546	23.938	22.526
	90	26.438	26.354	25.188	25.151	23.938	23.587
	120	26.438	26.643	25.188	25.465	23.625	24.156

3.4 Adsorption Thermodynamics

The adsorption thermodynamics data are as presented in Table 5. The thermodynamic parameters obtained for Congo red adsorption showed that all three hybrid adsorbents exhibit negative enthalpy values throughout the investigated temperature range (25-60 °C), confirming that the adsorption process is exothermic. The magnitude of ΔH^o falls within the typical range for physisorption mechanisms (-20 to -80 kJ/mol) (Wang *et al*., 2026). Entropy changes highlight the degree of order or disorder at the solid-solution interface. The entropy values are negative, implying increased order as dye molecules become immobilized on the adsorbent surface (Mohammad *et al*., 2015). The Gibbs free energy values provide a measure of spontaneity. The $\Delta G°$ values generally increase with temperature, indicating reduced spontaneity at higher temperatures. However, the magnitude of values of $\Delta G°$ indicates that the adsorption process is feasible for all the systems.

Table 5: Adsorption Thermodynamic Data

Temp (k)	Sample 2			Sample 3			Sample 4		
	ΔH^o (kJ/mol)	ΔS^o (J/mol k)	ΔG^o (kJ/mol)	ΔH^o (kJ/mol)	ΔS^o (J/mol k)	ΔG^o (kJ/mol)	ΔH^o (kJ/mol)	ΔS^o (J/mol k)	ΔG^o (kJ/mol)
323.15	-21.093	-73.74	1.113	-21.289	-77.012	1.654	-16.397	-63.710	3.242
328.15			1.347			2.316			2.621
338.15			1.859			3.219			3.837
348.15			3.032			3.871			4.582
358.15			3.813			4.604			5.229

4.0 CONCLUSION

This study has demonstrated that the Zeolite Y/Coconut Shell Activated Carbon hybrid adsorbents effectively removed the Congo red dye from aqueous solutions, recording removal efficiencies of 91.36%, 89.63% and 82.72 % for Samples 2, 3 and 4 respectively, at dosage of 0.8g/50ml, pH of 4, contact time of 60 mins and temperature of 25 ºC. Thus, Sample 3 was noted to exhibit intermediate performance due to its balanced composition. The adsorption process was found to follow Langmuir isotherm and Pseudo-second-order kinetics models. Thermodynamic studies revealed that Congo red adsorption revealed exothermic and non-spontaneous behaviour. However, the smaller values of ΔG° indicates that the adsorption process is feasible.

5.0 REFERENCES

Alawam, A.S., Mahgoub, S.M., Allam, A.A., Radalla, A.M., Shemy, M.H. & Mahmoud, R. (2025). Sustainable zeolite/activated carbon nanocomposite for dual-dye adsorption, kinetic and thermodynamic studies, and urea electrooxidation applications. RSC Adv., 15(51), 43983-44006. https://doi.org/10.1039/d5ra06559c

Arias, F.E., Tubon-Usca, G., Moreno-Samaniego, M., Penafiel-Ojeda, C., Corrente, G.A., Milone, C., Caputi, L.S. & Beneduci, A. (2026). Comparative adsorption of methylene blue on GO- and rGO-modified natural clinoptilolite: Role of carbon oxidation state and pore blocking. Journal of Material Science, 61, 7516-7544. https://doi.org/10.1007/s10853-026-12300-2

Ayawei, N., Ebelegi, A.N. & Wankasi, D. (2017). Modelling and Interpretation of Adsorption Isotherms. Hindawi Journal of Chemistry, Article ID 3039817. https://doi.org/10.1155/2017/3039817

Chakraborty, R., Asthana, A., Singh, A. K., Jain, B. & Susan, A.B.H. (2022). Adsorption of heavy metal ions by various low-cost adsorbents: a review. International Journal of Environmental Analytical Chemistry, 102(2), 1-38. https://doi.org/10.1080/03067319.2020.1722811

Deng, Z., Gu, S., Cheng, H., Xing, D., Twagirayezu, G., Wang, X., Ning, W. & Mao, M. (2022) Removal of Phosphate from Aqueous Solution by Zeolite-Biochar Composite: Adsorption Performance and Regulation Mechanism. Appl. Sci., 12, 5334. https://doi.org/10.3390/app12115334

Dryaz, A.R., Shaban, M., Al-Mohamadi, H., AbuAl-Ola, K.A., Hamd, A., Soliman N.K. & Ahmed, S.A. (2021). Design, characterization, and adsorption properties of Padina gymnospora/zeolite nanocomposite for Congo red dye removal from wastewater. Scientific Reports, 11:21058, https://doi.org/10.1038/s41598-021s-00025-y.

El Jery, A., Alawamleh, H.S.K., Sami, M.H., Abbas, H.A., Sh. Sammen, S., Ahsan, A., Imteaz, M.A., Shanableh, A., Shafiquzzaman, M., Osman, H. & Al-Ansari, N. (2024). Isotherms, kinetics and thermodynamic mechanism of methylene blue dye adsorption on synthesized activated carbon. Scientific Reports, 14:970. https://doi.org/10.1038/s41598-023-50937-0.

Fernandes de Magalhaes, L., Rodrigues da Silva, G. & Clark Peres, A.E. (2022). Zeolite Application in Wastewater Treatment. Adsorption Science & Technology, 1-26, https://doi.org/10.1155/2022/4544104

Gayathri, K., Saranraj, P., Nayak, A.K., Kesavardhini, K., Lokeshwari, B. & Cardoso, A.M. (2026). Microbial Innovations for Sustainable Wastewater Management: A Comprehensive Review of Azo Dye Bioremediation. Sustainability, 18, 3041. https://doi.org/10.3390/su18063041

Gkika, D.A., Tolkou, A.K., Katsoyiannis, I.A. & Kyzas, G.Z. (2025). The adsorption-desorption-regeneration pathway to a circular economy: The role of waste-derived adsorbents on chromium removal. Separation and Purification Technology, 368, 132996. https://doi.org/10.1016/j.seppur.2025.132996.

Jaramillo-Fierro, X., Alvarado, H., Montesdeoca, F. & Valarezo, E. (2023). Faujasite-Type Zeolite Obtained from Ecuadorian Clay as a Support of ZnTiO3/TiO2 NPs for Cyanide Removal in Aqueous Solutions. Int. J. Mol. Sci., 24, 9281. https://doi.org/10.3390/ijms24119281

Javeda, T., Thumma, A., Nur Uddin, A., Akhter, R., Babar Taj, M., Zafar, S., Baig, M.M., Ahmad Shah, S.S., Wasim, M., Abid, M.A., Masood, T., Jilani, M.I. & Batool, M. (2024). Batch adsorption study of Congo Red dye using unmodified Azadirachta indica leaves: isotherms and kinetics. Water Practice & Technology, 19(2), 546. doi: https://doi.org/10.2166/wpt.2024.020

Khan, N., Anwer, A.H., Khan, M.D., Azam, A., Ibhadon, A. & Khan, M.Z. (2021). Magnesium ferrite spinels as anode modifier for the treatment of Congo red and energy recovery in a single chambered microbial fuel cell. Journal of Hazardous Material, 410, 124561. https://doi.org/10.1016/j.jhazmat.2020.124561.

Mnyango, J.I., Nyoni, B., Phiri, C., Fouda-Mbanga, B.G., Amusat, S.O., Maringa, A., Yalala-Ndlovu, B., Hlabano-Moyo, B., Tywabi-Ngeva, Z. & Hlangoth, S.P. (2025). Sustainable wastewater treatment: Mechanistic, environmental, and economic insights into biochar for synthetic dye removal. Next Materials, 9, 100974, https://doi.org/10.1016/j.nxmate.2025.100974

Mohamed, F., Shaban, M., Zaki, S.K., Abd-Elsamie, M.S., Sayed, R., Zayed, M., Khalid, N., Saad, S., Omar, S., Ahmed, A.M., Abanoub Gerges, H.R., El-Mageed, A. & Soliman, N.K (2022). Activated carbon derived from sugarcane and modified with natural zeolite for efficient adsorption of methylene blue dye: Experimentally and theoretically

approaches', Science Reports, 12:18031, https://doi.org/10.1038/s41598-022-22421-8.

Mohammad, Y.S., Shaibu-Imodagbe, E.M., Igboro, S.B., Giwa, A. & Okuofu, C.A. (2015). Isotherm, kinetics and thermodynamics of phenol adsorption onto rice husk activated carbon. Leonardo Electronic Journal of Practices and Technologies, 26, 115-128. http://lejpt.academicdirect.org

Nwafulugo, F.U. (2014). Application of Zeolite 4A-Metakaolin Matrix for the Removal of Some Heavy Metals from Crude Oil Tank Farm Wastewater. Ph.D Dissertation, Ahmadu Bello University, Zaria. Nigeria.

Olatunji, M.A., Salam, K.A. & Evuti, A.M. (2024). Simultaneous Adsorption of Aqueous Pb2+, Cu2+, Zn2+, and Cd2+ Using Surfactant-Modified and Unmodified Activated Carbon in a Fixed Bed Column. Journal of Encapsulation and Adsorption Sciences, 12, 1-24. https://www.scirp.org/journal/jeas

Onigemo, M.T., Balogun, A.A., Odeh, L.U., Udoh, E.A., Mohammed, A., Omolusi, A.R., Ankomah, N.O., Akyea Mensah, S.B., Onele, E.J. & Akoh, M.D. (2024). Production and Characterization of Activated Carbon from Coconut Shell for Adsorption of Lead (II) Ion from Waste Water. Adv. J. Chem. B: Nat. Prod. Med. Chem, 6, 269-283. doi: https://doi.org/10.48309/AJCB.2024.472061.1240.

Oyedoh, E.A. & Igbokwe, O.P. (2025). Evaluation of novel NaOH/activated carbon/zeolite biocomposite as an efficient adsorbent for oilfield produced water treatment. South African Journal of Chemical Engineering, 51, 302-314. https://doi.org/10.1016/j.sajce.2024.12.006.

Schmidt, C., Berghahn, E., Ilha, V. & Granada, C.E. (2019). Biodegradation potential of Citrobacter cultures for the removal of amaranth and congo red azo dyes. International Journal of Environmental Science and Technology, 16, 6863-6872. http://doi.org/10.1007/s13762-019-02274-x.

Şenol, Z.M., Ertap, E., Fernine, Y. & El Messaoudi, N. (2024). Adsorptive removal of synthetic dye from its aqueous solution by using chitosan-bentonite composite: DFT and experimental studies. Polymer Bulletin, 81:12795–12817. https://doi.org/10.1007/s00289-024-05323-9

Tan, I.A.W., Abdullah, M.O., Lim, L.L.P. & Yeo, T.H.C. (2017). Surface Modification and Characterization of Coconut Shell-Based Activated Carbon Subjected to Acidic and Alkaline Treatments. Journal of Applied Science & Process Engineering, 4(2), 186-194. https://doi.org/10.33736/jaspe.435.2017

Tubon-Usca, G., Centeno, C., Pomasqui, S., Beneduci, A. & Arias, F.A. (2025). Enhanced Adsorption of Methylene Blue in Wastewater Using Natural Zeolite Impregnated with Graphene Oxide. Appl. Sci., 15, 2824. https://doi.org/10.3390/app15052824

Wang, Q., Xu, Y., Yu, J., Xia, R., Jiang, Z., Zhang, Y. & Xiong, F. (2026). Efficient and Rapid Removal of Cationic Methylene Blue from Aqueous Solution by Alkali-Treated Bamboo Powders as Biosorbents. Separations, 13, 57. https://doi.org/10.3390/separations13020057

Wongcharee, S., Aravinthan, V. & Erdei, L. (2018). Mesoporous activated carbon-zeolite composite prepared from waste macadamia nut shell and synthetic faujasite. Chinese Journal of Chemical Engineering. doi: https://doi.org/10.1016/j.cjche.2018.06.024

Xiong, Z., Zheng, H., Hu, Y., Hu, X., Ding,W., Ma, J. & Li, Y. (2021). Selective adsorption of Congo red and Cu(II) from complex wastewater by core-shell structured magnetic carbon zeolitic imidazolateframeworks-8 nanocomposites. Separation and Purification Technology. doi: https://doi.org/10.1016/j.seppur.2021.119053